# Adsorption and Reaction of Acetaldehyde on Stoichiometric and Defective $SrTiO_3$(100) Surfaces

**Li-Qiong Wang* and Kim F. Ferris**

*Material Science Division, Pacific Northwest National Laboratory, Richland, Washington 99352*

**Samina Azad, Mark H. Engelhard, and Charles H. F. Peden**

*Chemical Sciences Division, Pacific Northwest National Laboratory, Richland, Washington 99352*

*Received: July 25, 2003; In Final Form: November 17, 2003*

The adsorption and reaction of acetaldehyde ($CH_3CHO$) on stoichiometric ($TiO_2$-terminated) and reduced $SrTiO_3$(100) surfaces have been investigated using temperature-programmed desorption (TPD) and X-ray photoelectron spectroscopy (XPS). Acetaldehyde adsorbs molecularly on the stoichiometric $SrTiO_3$(100) surface that contains predominately $Ti^{4+}$ cations. The $Ti^{4+}$ sites on the stoichiometric $SrTiO_3$(100) surface are not sufficiently active for surface reactions such as aldol condensation, as opposed to the $Ti^{4+}$ ions on the $TiO_2$-(001) surface. However, decomposition and redox reactions of acetaldehyde occur in the presence of surface defects created by $Ar^+$ sputtering. The decomposition products following reactions of acetaldehyde on the defective surface include $H_2$, $C_2H_4$, CO, $C_4H_6$, and $C_4H_8$. Reductive coupling to produce $C_2H_4$ and $C_4H_8$ is the main reaction pathway for decomposition of acetaldehyde on the sputter-reduced $SrTiO_3$(100) surface.

## 1. Introduction

The adsorption and reaction of oxygenated hydrocarbons on metal oxide surfaces are of much interest from both fundamental and practical perspectives. The chemistry of oxygenated hydrocarbons on metal oxides is rich and complex, involving a variety of catalytic processes such as selective oxidation, alcohol synthesis, reduction, condensation, etherification, and gasoline production from methanol. The reactivity of these catalytic processes largely depends on the characteristics of the oxide catalysts defined by their surface structures, acid−base properties, and surface defects. Another very important aspect of the investigation of the reactions of oxygenated hydrocarbons on metal oxide surfaces is the pressing environmental concerns related to the hazardous products in automobile exhaust gases. Oxygenated hydrocarbons are often used as fuels and fuel additives,[1−3] and they may be formed as a result of incomplete combustion of fuel in the engine. Among several families of oxygenates, aldehydes are particularly undesirable in exhaust because of their potential carcinogenic effects.[4] To efficiently reduce these toxic exhaust products, it is especially helpful to have a fundamental understanding of the adsorption and reactions of aldehydes on oxide surfaces. Because of the complexities in the chemistry of aldehydes on oxides such as $CeO_2$, $TiO_2$, MgO, CaO, $SnO_2$, and $Al_2O_3$, studying the reactions of simple aldehydes, such as formaldehyde or acetaldehyde, on well-defined model oxide surfaces is essential.

Both $TiO_2$ and $SrTiO_3$ single crystals have been widely used as model surfaces to study oxide surface chemistry because of their availability as well as the varieties of oxidation states and coordination environments they provide. Oxygen vacancies or other more complex surface defects associated with the reduced states of these materials can be introduced to the surface by either heat treatment or argon-ion bombardment, both of which preferentially remove near-surface oxygen atoms.[5]

Previous studies reported interactions of acetaldehyde on single-crystal $TiO_2$(001) surfaces under ultrahigh vacuum (UHV).[6−9] The formation of carbon−carbon bonds on these surfaces was obtained by aldol condensation or by reductive-coupling routes. The decomposition of acetaldehyde and formation of C-4 products on both {011}- and {114}-faceted $TiO_2$(001) surfaces follow the mechanism of aldol condensation producing crotonaldehyde and crotyl alcohol.

$SrTiO_3$ surfaces have attracted a considerable amount of attention because of their photocatalytic properties and their important role in the photoelectrolysis of water under illumination with band gap radiation even in the absence of an applied bias.[10] Although, as noted above, the reactions of acetaldehyde have been investigated extensively on $TiO_2$ surfaces, they have not been studied on $SrTiO_3$ surfaces. $SrTiO_3$(100) was chosen as the model surface in this study not only because of its heterogeneous and photocatalytic activities but also because the investigations of reactions of oxygenated hydrocarbons on a well-defined single-crystal mixed-oxide surface, such as $SrTiO_3$, are few. $SrTiO_3$(100) surfaces have two possible nonpolar surface terminations: a SrO-terminated surface and a $TiO_2$-terminated surface. This study focuses on the interaction of acetaldehyde with the $TiO_2$-terminated oxidized and reduced $SrTiO_3$(100) surfaces. The surface structures of the fully oxidized $TiO_2$(110), $TiO_2$(100), and $TiO_2$-terminated $SrTiO_3$-(100) are schematically illustrated in Figure 1. As compared with $TiO_2$(110) and (100) surfaces, the $TiO_2$-terminated $SrTiO_3$-(100) surface shows a unique geometric arrangement of the surface Ti and O atoms. The latter surface is relatively flat with only in-plane oxygen atoms, whereas the $TiO_2$(110) and $TiO_2$-(100) surfaces have rows of two-coordinate bridging oxygen atoms lying above the rows of Ti atoms (Figure 1). Thus, by studying the $TiO_2$-terminated $SrTiO_3$(100) surfaces, we explore

* Author to whom correspondence should be addressed. E-mail: lq.wang@pnl.gov.

10.1021/jp030917v CCC: $27.50 
Published on Web 01/07/2004

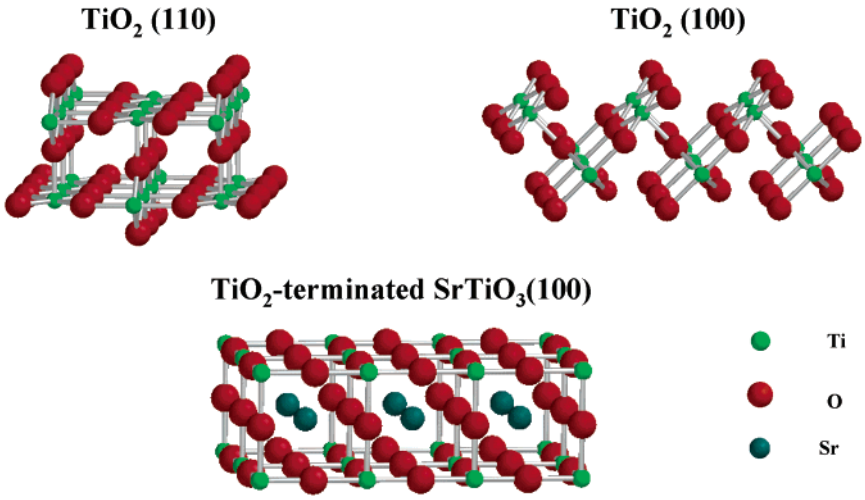


**Figure 1.** Schematic models for the $TiO_2$(110), $TiO_2$(100), and $TiO_2$−terminated $SrTiO_3$(100) surfaces.

the opportunities to further investigate the influence of Ti and O atomic arrangements and bonding configurations on this surface, as well as the effect of the bridging oxygen atoms on the adsorption and reaction of acetaldehyde. In this study we compare the results obtained from the $TiO_2$-terminated $SrTiO_3$-(100) surface with those obtained from the $TiO_2$ surfaces. Because different reaction pathways were chosen for carbon−carbon bond formation during the reactions of acetaldehyde on stoichiometric and reduced $TiO_2$(001) surfaces, it is also interesting to study the influence of the reduced Ti states on the reactions of acetaldehyde on $SrTiO_3$(100) surfaces.

## 2. Experimental Section

The $SrTiO_3$(100) crystals ($10 \times 10 \times 2$ mm$^3$, with a $Ti^{4+}$ surface density of $6.55 \times 10^{14}$ atoms/cm$^2$) were purchased from Princeton Scientific. The crystal used for temperature-programmed desorption (TPD) measurements was epi-polished on both sides and cut with 0.5 mm × 2.0 mm slots around the four sides of the crystals. The crystal was mounted on a polished tantalum plate with a 0.025-mm thick gold foil sandwiched between the two surfaces. Chromel−alumel thermocouple wires were glued to the sample using a ceramic glue before the sample was transferred to the TPD chamber (detailed descriptions of the crystal mounting have been published previously).[11] The sample can be resistively heated to 1000 K and cooled to 120 K by thermal contact with a liquid nitrogen filled reservoir. The samples were cleaned by $Ar^+$ sputtering and by subsequent vacuum annealing at high temperatures (850 K). The stoichiometric surfaces were then obtained by annealing at 800−850 K for 10 min in $1 \times 10^{-7}$ Torr $O_2$. The reduced surfaces used for TPD measurements were prepared by $Ar^+$ bombardment at 2 keV for 20 min. The samples were dosed via backfilling the chamber with the reactant gases, and the measured pressures were not corrected for ionization gauge sensitivities. The cleanliness of the samples was verified by Auger electron spectroscopy (AES) measurements prior to the TPD and X-ray photoelectron spectroscopy (XPS) experiments.

TPD studies were performed in an ultrahigh vacuum (UHV) system containing a single pass cylindrical mirror analyzer for AES, a quadrupole mass spectrometer for TPD, optics for low-energy electron diffraction (LEED), and a sputter gun for sample cleaning. In the TPD experiments the desorbing species were detected by use of a UTI quadrupole mass spectrometer (QMS) interfaced to a personal computer (PC) allowing nine masses to be monitored simultaneously during the desorption sweep. To minimize spurious signals, the mass spectrometer was enclosed in a shroud with a 1-mm diameter hole in the front. TPD measurements were performed by positioning the crystal in front of the QMS and using a linear temperature ramp of 2.5 K/s.

XPS measurements were made in a Physical-Electronics Quantum 2000 scanning ESCA (electron spectroscopy for chemical analysis) microprobe system using a hemispherical analyzer. Monochromatic Al Kα X-rays (1486.7 eV), with an X-ray spot size of 1.5 mm × 0.2 mm, were used to generate the spectra. In these experiments the base pressure of the system was about $2 \times 10^{-10}$ Torr. Multiplex data were collected with a pass-energy of 23.5 eV and were referenced to an energy scale with binding energies for Au 4f at 84 ± 0.03 eV and Cu $2p_{3/2}$ at 932.67 ± 0.03 eV.

Acetaldehyde (>99.5% pure, ACS reagent grade) was obtained from Aldrich. Several freeze−pump−thaw cycles with liquid nitrogen were performed on the acetaldehyde sample prior to the TPD experiments. Various exposures of acetaldehyde were dosed through a leak valve to the crystal at ~120 K during the TPD studies. It is difficult to correlate the reactant gas exposures to the exact surface coverage in the absence of a calibrated dosing source. Thus, in this study a 1-Langmuir exposure (1 L) may not necessarily provide a 1-ML (monolayer) acetaldehyde dose to the surface.

## 3. Results and Discussion

**3.1. Interaction of Acetaldehyde with Stoichiometric $SrTiO_3$(100) Surfaces.** Fully oxidized $SrTiO_3$(100) surfaces, prepared in our studies by sputtering followed by annealing at 800−850 K in $O_2$, show a 1 × 1 LEED pattern. Previous ion scattering studies[12,13] have shown that similarly prepared $SrTiO_3$-(100) single-crystal surfaces were predominantly terminated by $TiO_2$ atomic planes. Thus, the stoichiometric or fully oxidized $SrTiO_3$(100) surfaces used in our studies should be mostly $TiO_2$-terminated. Figure 2 displays a series of 29 amu TPD spectra that monitor desorption of $CH_3CHO$, following adsorption of 0.1 L (a), 0.5 L (b), 1 L (c), 2 L (d), and 6 L (e) of $CH_3CHO$ on a fully oxidized $SrTiO_3$(100) at 120 K. Spectrum a in Figure 2 contains two distinct peaks indicating desorption of acetaldehyde from this surface at 210 and 273 K. The 273 K TPD feature with its long tail extending up to 350 K grows in intensity and shifts to lower temperatures with increasing exposures of $CH_3CHO$ to the oxidized surface. As shown in Figure 2, this 273 K feature shifts to 247 K for 0.5 L of $CH_3CHO$ (spectrum

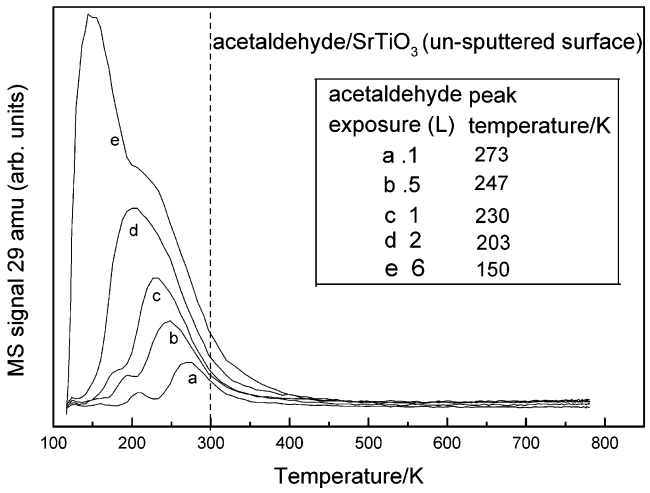


**Figure 2.** TPD spectra of 29 amu for (a) 0.1 L, (b) 0.5 L, (c) 1 L, (d) 2 L, and (e) 6 L of $CH_3CHO$ adsorbed on a fully oxidized $TiO_2$-terminated $SrTiO_3(100)$ at 120 K. The dashed vertical line at 300 K is drawn to help the explanation of the text.

b) and to 230 K for 1 L of $CH_3CHO$ (spectrum c) on the same surface. The small 210 K TPD feature (spectrum a) shifts to lower temperatures as well, but its intensity only increases slightly with the increasing exposures of acetaldehyde (up to 1 L) on this surface. However, spectra d and e in Figure 2, for acetaldehyde exposures of 1 L and above, exhibit significant increases in the intensities of this lower temperature feature. Upon exposure of 2 L of acetaldehyde to the oxidized surface, the two desorption features overlap resulting in a relatively broad peak centered at ~200 K. A further increase in exposure to 6 L produces a sharp desorption peak at 150 K with a shoulder at 200 K.

We assign the desorption feature, that shifts from 273 to 230 K in spectra a−c in Figure 2, to the chemisorbed molecular state of $CH_3CHO$ bound to a $Ti^{4+}$ cation site. The large shift with increasing coverage is presumably due to the repulsive interactions between adsorbed $CH_3CHO$ molecules. The smaller desorption feature that shifts from 210 to 180 K, (spectra a−c, Figure 2) is most likely due to the desorption of weakly bound $CH_3CHO$ from a second layer, indicating that accumulation of the second layer of $CH_3CHO$ occurs before the completion of the first layer on the oxidized surface. The 150 K feature (spectrum e) is attributed to the multilayer desorption since this feature continues to grow with increasing exposures of acetaldehyde on this surface.

On the basis of a simple Redhead analysis[14] assuming a pre-exponential factor of $1 \times 10^{13}$ $s^{-1}$, we estimate a first-order desorption energy of ~13.5 kcal/mol for desorption of $CH_3CHO$ from the fully oxidized $SrTiO_3(100)$ surfaces at a coverage close to the saturation of a monolayer. First principles electronic structure calculations for formaldehyde adsorption would indicate a 14.4 kcal/mol binding energy, comparable to the Redhead analysis value for acetaldehyde. Details of these calculations will be reported separately.[15] The binding nature of $CH_3CHO$ depends on the kind of chemical interaction and the effect of the $sp^2$ oxygen hybridization as opposed to the $sp^3$ oxygen hybridization found in water, methanol, or ethanol. Schematic adsorption geometries for acetaldehyde, methanol, and ethanol on $TiO_2$-terminated $SrTiO_3(100)$ surfaces are illustrated in Figure 3. Acetaldehyde adsorbs onto the $SrTiO_3(100)$ surface with the oxygen atom bound to the $Ti^{4+}$ site, whereas the $-CH_3$ group is placed away from the surface. In addition to the weak acid−base interaction between $CH_3CHO$ and the $SrTiO_3$ surfaces, weak electrostatic and dipolar interactions may exist between the α-hydrogen of the tilted $CH_3CHO$ molecules and one or more surface oxygen atoms. The binding between $CH_3CHO$ and the surface would be reduced by a repulsive interaction of methyl groups with the surface. Because $H_2O$, $CH_3OH$, and $CH_3CH_2OH$ are stronger bases (and show $sp^3$ oxygen hybridization) than acetaldehyde ($sp^2$), they exhibit stronger interactions with the strontium titanate surface. Electronic structure studies have

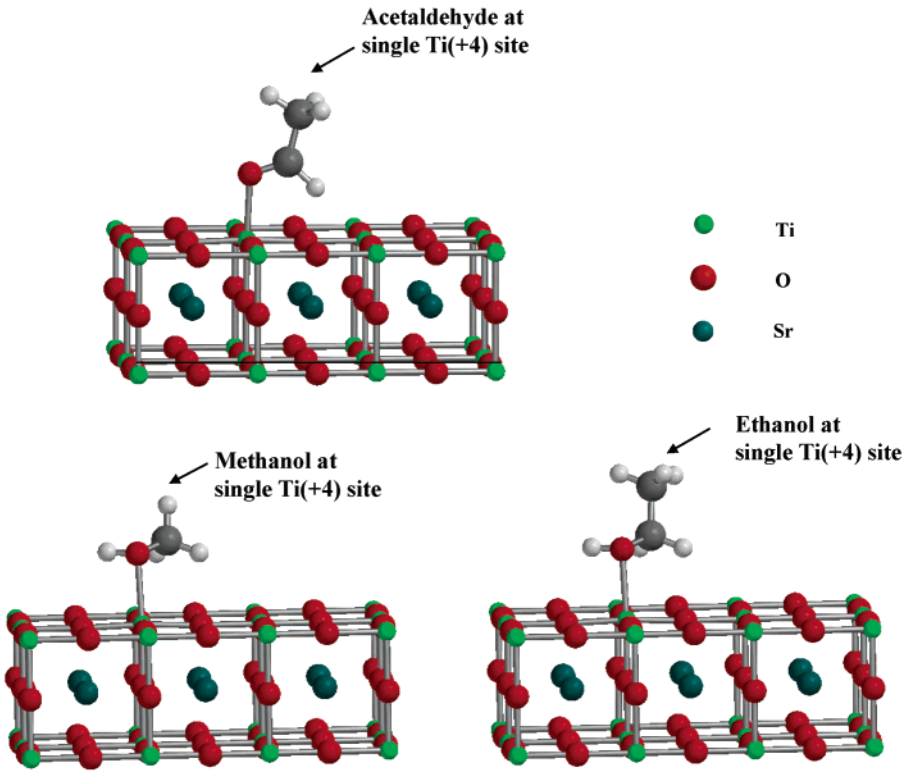


**Figure 3.** Schematic illustrations of the adsorption geometries for acetaldehyde, methanol, and ethanol on $TiO_2$-terminated $SrTiO_3(100)$ surfaces.

given binding energies of 19.1 and 19.4 kcal/mol for water and methanol on stoichiometric $SrTiO_3$(100) surfaces,[15] respectively. Our TPD data has shown that the interaction of $SrTiO_3$(100) with $H_2O$ is marginally weaker than the interactions with $CH_3OH$ and $CH_3CH_2OH$.[15] For both $CH_3OH$ and $CH_3CH_2OH$ adsorption onto the $TiO_2$-terminated $SrTiO_3$(100) surface, multiple surface−adsorbate proton interactions are possible: one proton from the $-OH$ group and two others from the $-CH_3$ group in $CH_3OH$ or the $-CH_2$ group in $CH_3CH_2OH$ lie approximately on the same plane above the $SrTiO_3$(100) surface, enhancing the attractive interaction between the surface and the adsorbates (shown in Figure 3).

Unlike the stable bulk-terminated $SrTiO_3$(100), $TiO_2$(110), and $TiO_2$(100) surfaces shown in Figure 1, the $TiO_2$(001) surface is unstable and facets upon annealing to produce a variety of unsaturated coordinates as a result of simple bulk termination in the (001) plane.[16−20] Because of the stability of the (110) and (100) planes of $TiO_2$, more surface science studies have been reported on the $TiO_2$(110) and $TiO_2$(100) surfaces compared to similar studies on the $TiO_2$(001) surfaces. It is interesting to note, however, that the previous TPD studies of acetaldehyde on $TiO_2$ single-crystal surfaces[6] were performed only on the {011}- and {114}-faceted $TiO_2$(001) surfaces at 300 K, and the corresponding {011}- and {114}-faceted structures produced by annealing to higher temperatures were observed by low-energy electron diffraction (LEED).[16,17] Scanning tunneling microscopy (STM) images[21] displayed the predominant (011) and stepped (011) planes in addition to a small number of (114) and (111) planes on the annealed (700−800 K) $TiO_2$(001) surfaces. Although the (011) planes contain only one type of Ti atom (five-coordinated $Ti^{4+}$), the {011}-faceted $TiO_2$(001) surface contains a variety of unsaturated Ti sites due to the presence of the (114), (111), and stepped (011) planes on this surface. Annealing this surface to 900−1000 K results in the {114}-faceted structure as observed in a recent STM study.[22] Because the {114}-faceted surfaces are obtained by high-temperature annealing in UHV, they are relatively more reduced compared to the {110}-faceted surfaces and contain a wider range of sites including four- and five-coordinated Ti sites.

Because the faceted $TiO_2$(001) surface is composed of a large variety of sites, it is difficult to directly compare our results on the fully oxidized $SrTiO_3$(100) surfaces with the previous studies of acetaldehyde on $TiO_2$(001) surfaces.[6] However, a comparison between TPD spectra for $H_2O$ on fully oxidized $SrTiO_3$(100), $TiO_2$(110), and (1 × 1) $TiO_2$(100) surfaces can provide some useful information related to the bonding and reaction pathways of acetaldehyde on these surfaces. As discussed earlier, the geometric structure of the $TiO_2$-terminated $SrTiO_3$(100) surface is considerably different than those of $TiO_2$(110) and $TiO_2$(100) surfaces. Notably, there are rows of bridging oxygen atoms on the $TiO_2$(110) and (1 × 1) $TiO_2$(100) surfaces, whereas the $SrTiO_3$(100) surface with a $TiO_2$-termination is relatively flat with only in-plane oxygen atoms on the surface.

A comparison of our previous water TPD results obtained from these surfaces has shown that water molecules exhibit relatively stronger binding to the $TiO_2$(110) and $TiO_2$(100) surfaces than to the $SrTiO_3$(100) surface.[23] The nature of the $Ti^{4+}$ cation sites was found to be more covalent on the $TiO_2$-terminated $SrTiO_3$(100) compared to the same sites on the $TiO_2$ surfaces based on electronic structural calculations,[24,25] and these differences can be attributed primarily to the influence of the Sr cations on the electronic structure of the Ti cations in the mixed oxide of $SrTiO_3$. In particular, as was proposed in previous calculations on the energetics of mixed metal oxide surfaces, in the mixing of two oxides (one having a more ionic cation than the other), the ionic properties of the more ionic cation are expected to increase further, while the covalent properties of the more covalent ion should also be enhanced.[24,25] Because Sr is a more ionic cation than Ti, Sr is more ionic in $SrTiO_3$ than in SrO and Ti is more covalent in $SrTiO_3$ than in $TiO_2$. Thus, either the higher covalence or weaker acidity of $Ti^{4+}$ cations on $SrTiO_3$(100) surfaces results in a weaker acid−base interaction between $Ti^{4+}$ sites and water. The absence of the bridging oxygen atoms on the $SrTiO_3$(100) surface, that serve to aid the binding of water via hydrogen bonding, may also be partially responsible for the weaker adsorption of $H_2O$ on $SrTiO_3$(100). Both of these attributes of the $TiO_2$-terminated $SrTiO_3$(100) surface would suggest a weaker binding interaction between water and this surface compared to similar interactions on the $TiO_2$(110) and (1 × 1) $TiO_2$(100) surfaces.

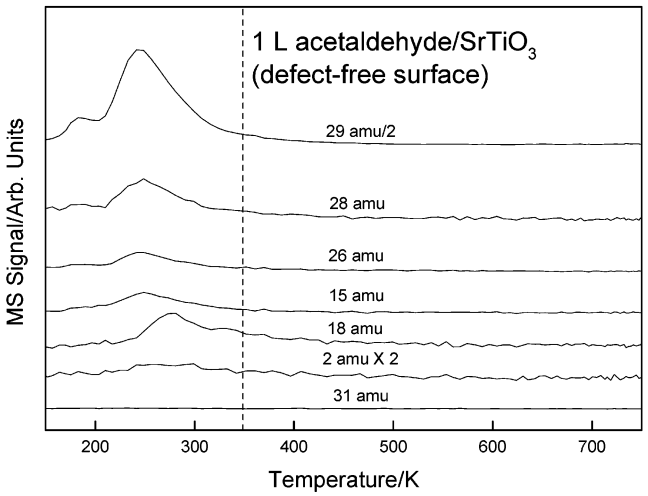


**Figure 4.** TPD spectra monitoring 2, 15, 18, 26, 28, 29, and 31 amu, following adsorption of 1 L of acetaldehyde exposure to the $TiO_2$-terminated stoichiometric $SrTiO_3$(100) surfaces at 120 K. The vertical line (dashed line) at 400 K is shown to divide the TPD features at temperatures above and below 400 K. The dashed vertical line at 350 K is drawn to help the explanation of the text.

The geometric structures of the $TiO_2$-terminated $SrTiO_3$(100), $TiO_2$(110), and $TiO_2$(100) surfaces are also responsible for the differences in dissociative $H_2O$ adsorption. It was found that water adsorbs dissociatively on 1 × 1 $TiO_2$ (100) but nondissociatively on $TiO_2$-terminated $SrTiO_3$(100) surfaces.[23] Our previous electronic structure calculations for $H_2O$ on $TiO_2$(110) and $TiO_2$(100) surfaces revealed that the dissociation of water molecules is more facile on the latter surface because of multiple hydrogen-bonding interactions with nearby bridging oxygen atoms.[26] On the basis of the water work, we would assume that acetaldehyde binds more strongly and exhibits higher reactivity on $TiO_2$ surfaces compared to that on the $TiO_2$-terminated $SrTiO_3$(100) surface.

Figure 4 displays TPD spectra monitoring 2, 15, 18, 26, 28, 29, and 31 amu, following adsorption of 1 L of acetaldehyde on the $TiO_2$-terminated stoichiometric $SrTiO_3$(100) surfaces at 120 K. For acetaldehyde on an oxidized $SrTiO_3$(100) surface no desorption products are observed at temperatures above 400 K, indicating that acetaldehyde does not decompose on the $TiO_2$-terminated $SrTiO_3$(100) surface when adsorbed at 120 K. At temperatures lower than 300 K, acetaldehyde ($m/e$ = 29 amu) desorbs molecularly from this surface as observed in Figure 4. The small desorption features for 28 and 26 amu match the fragmentation pattern of the parent acetaldehyde ($m/e$ = 29) molecule suggesting molecular desorption of acetaldehyde from the oxidized surface. No desorption features were observed for

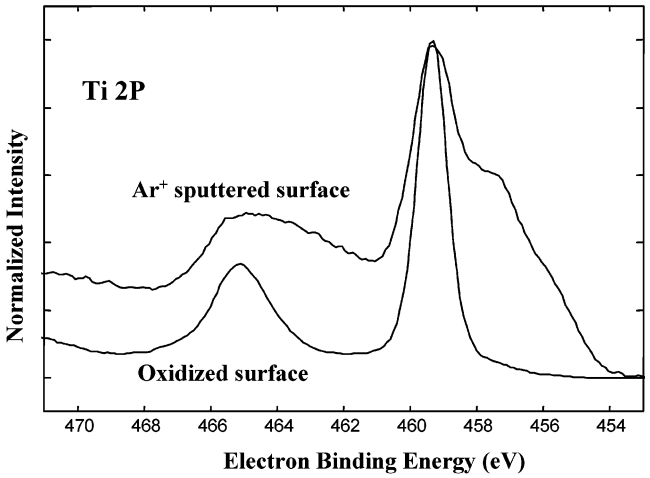


**Figure 5.** Ti 2p and O 1s XPS spectra for a sputter-reduced $SrTiO_3$-(100) surface and a nearly defect-free (stoichiometric) $SrTiO_3$(100) surface at 297 K.

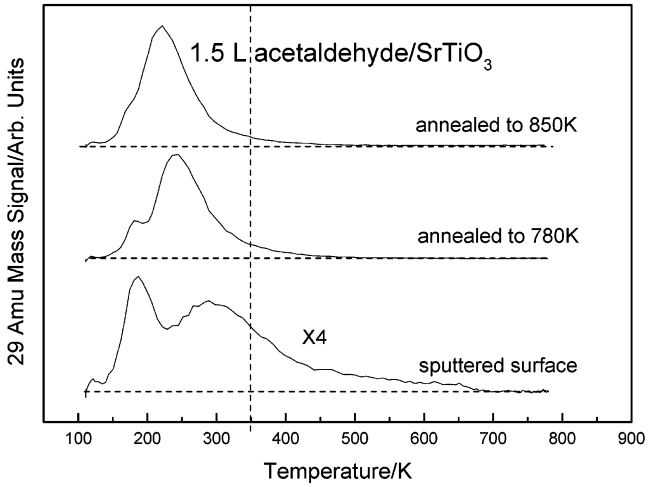


**Figure 6.** TPD spectra of 29 amu following adsorption of 1.5 L of acetaldehyde at 120 K on (a) the freshly sputtered $SrTiO_3$(100), (b) the same surface annealed at 780 K, and (c) the same surface annealed at 850 K. The dashed vertical line at 350 K is drawn to help the explanation of the text.

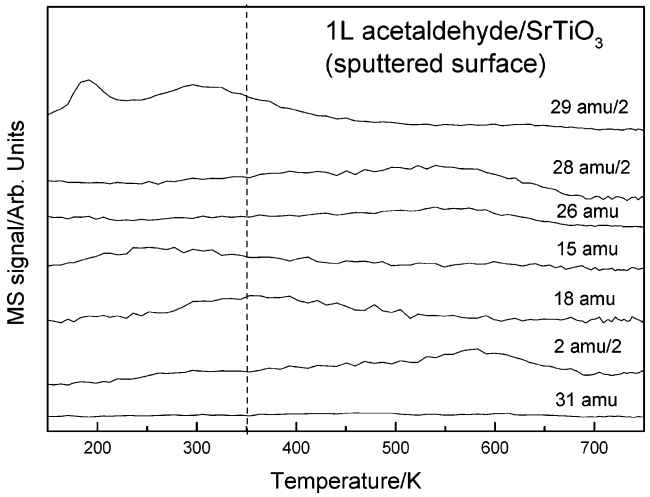


**Figure 7.** TPD spectra monitoring 2, 15, 18, 26, 28, 29, and 31 amu following adsorption of 1 L of acetaldehyde on the sputter-reduced $SrTiO_3$(100) surface at 120 K. The dashed vertical line at 350 K is drawn to help the explanation of the text.

TPD spectra monitoring higher masses ($m/e$ = 39, 42, 54, 56, 58, 68, 70, and 72 amu) suggesting that carbon−carbon bond formation does not take place on the oxidized $SrTiO_3$(100) surfaces. The small water TPD peak shown in Figure 4 is related to the desorption of the background water in the system, as the same desorption state of water can be obtained from a blank TPD run (without dosing with acetaldehyde).

The basicity of aldehydes is between that of alcohols and carboxylic acids, making it interesting to compare the reactivity between alcohols, aldehydes, and carboxylic acids. Our studies showed that methanol, ethanol, and acetaldehyde mostly adsorb molecularly,[15] whereas formic acid exhibits dissociative adsorption on the stoichiometric $SrTiO_3$(100) surface.[27] The initial dissociated formate species on $SrTiO_3$(100) attaches to Ti cations sites with bidentate binding with decomposition products obtained during TPD that include CO, $CO_2$, and $H_2O$. The reactivity of HCOOH on the $SrTiO_3$(100) surface[27] is similar to that on the $TiO_2$ surfaces.[28−31] Acetaldehyde, methanol, and ethanol show lower adsorption energies and reactivity on $SrTiO_3$(100) as compared with those on $TiO_2$ surfaces.[15,32,33] Therefore, it is apparent that the adsorption and dissociation of weaker acids such as methanol, ethanol, and acetaldehyde are largely influenced by the geometric and electronic structures of oxide surfaces.

**3.2. Interaction of $CH_3CHO$ with Reduced $SrTiO_3$(100) Surfaces.** $Ar^+$ bombardment causes structural and chemical modifications at the surface and near-surface regions. In our studies XPS measurements indicated that sputtering the $TiO_2$-terminated $SrTiO_3$(100) surface with $Ar^+$ ions was an effective way to systematically shift the average surface oxidation state from $Ti^{4+}$ to $Ti^{3+}$. As depicted in Figure 5, the XPS spectrum of a fully oxidized $SrTiO_3$(100) surface contains a narrow and symmetric Ti 2p peak that results predominantly from $Ti^{4+}$ cations on the surface and near-surface region. The significantly reduced surface prepared by $Ar^+$ sputtering shows a large broadening in the spin−orbit split Ti 2p peaks to lower binding energy which is due to the presence of reduced Ti cations (mostly $Ti^{3+}$ and $Ti^{2+}$ cations). These results are consistent with more detailed XPS studies on the oxidized and reduced $SrTiO_3$ surfaces that we have published previously.[23,27]

Figure 6 displays the TPD spectra monitoring mass 29 amu following adsorption of 1.5 L of $CH_3CHO$ at 120 K on fully oxidized and annealed (780 and 850 K) $SrTiO_3$(100) surfaces. These spectra are essentially identical to those obtained for a similar coverage of $CH_3CHO$ on the freshly oxidized surface shown in Figure 2. The TPD spectrum for $CH_3CHO$ on the freshly sputtered surface, also displayed in Figure 6, shows two desorption peaks at 180 K and at 300 K, where the 300 K feature has a long tail that continues all the way up to 650 K. The relatively high desorption temperature and the long tail indicates partial dissociation of $CH_3CHO$ on the sputter-reduced surface. Increasing the annealing temperatures reduces the dissociativity of the adsorbed $CH_3CHO$ molecules. The dissociation of the adsorbates can be associated with surface defects or oxygen vacancies created by $Ar^+$ sputtering.

A comparison of the TPD spectra for a number of desorption products observed following adsorption of $CH_3CHO$ on the oxidized (Figure 4) and reduced (Figure 7) $SrTiO_3$(100) surfaces clearly indicates differences in the reactivity of these two surfaces. As displayed in Figure 4 and Figure 7, which both monitor the same masses following adsorption of acetaldehyde on the oxidized and sputter-reduced surfaces, the desorption products include $H_2$ ($m/e$ = 2 amu), CO ($m/e$ = 28 amu), and $C_2H_4$ ($m/e$ = 28, 26 amu). On the reduced surface (Figure 7) these products are observed at temperatures above 400 K,

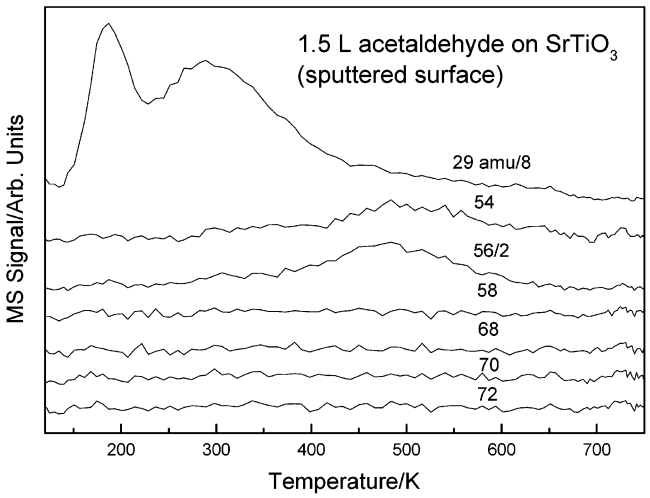


**Figure 8.** TPD spectra monitoring 29, 54, 56, 58, 68, 70, and 72 amu following adsorption of 1.5 L of acetaldehyde on the sputter-reduced $SrTiO_3$(100) surface at 120 K.

whereas the TPD spectra for $CH_3CHO$ on the oxidized surface show these masses only as cracking fragments of the parent $CH_3CHO$ molecules that are adsorbed molecularly on the surface. It is obvious from these results that the oxidized $SrTiO_3$-(100) surfaces cannot induce decomposition reactions of $CH_3$-CHO, whereas the reduced surfaces are highly reactive, suggesting that defects enhance the surface reactivity.

The TPD spectra in Figure 8, that monitor higher masses following adsorption of $CH_3CHO$ on the sputter-reduced surface at 120 K, clearly indicate carbon−carbon bond formation on this surface. Desorption of $C_4H_6$ (54 amu) and $C_4H_8$ (56 amu) are apparent in these spectra (Figure 8). Desorption of other probable reaction products such as ethanol ($C_2H_5OH$, $m/e$ = 31 amu), crotonaldehyde ($CH_3CH{=}CHCHO$, $m/e$ = 70 amu), and crotyl alcohol ($CH_3CH{=}CHCH_2OH$, $m/e$ = 72 amu) were not observed following adsorption of acetaldehyde on the reduced surface.

On the basis of the previous study of acetaldehyde on the reduced $TiO_2$(001) surface,[8] reductive coupling followed by the production of olefins may be the main reaction channel for reactions of acetaldehyde on the sputter-reduced $SrTiO_3$(100) surface. Equations 1 and 2 illustrate the proposed reaction pathways for the reductive coupling of $CH_3CHO$ on the reduced surface (here "g" and "a" stand for "gas" and "adsorbate", respectively, and $Ti^{3+}$ used here represents reduced cations created by $Ar^+$ sputtering).

$$2CH_3CHO(a) \rightarrow C_2H_4(g) + 2H_2(a) + 2CO(g) \quad (1)$$

$$2CH_3CHO(a) \rightarrow C_4H_8(g) + 2O(a) \quad (2)$$

$$2CH_3CHO(a) + 4Ti^{3+}(a) \rightarrow C_4H_8(g) + 4Ti^{4+}(a) + 2O^{2-}(a) \quad (3)$$

Reaction 1 represents a bimolecular reductive coupling that produces $C_2H_4$ ($m/e$ = 28, 27, 26 amu), CO ($m/e$ = 28 amu), and $H_2$ ($m/e$ = 2 amu), as observed in our TPD spectra (Figure 7). The 28 amu TPD spectrum (Figure 7) may be related to the desorption of CO ($m/e$ = 28 amu) and $C_2H_4$ ($m/e$ = 28 amu). The desorption of $C_4H_8$ ($m/e$ = 56 amu) indicates bimolecular coupling (shown in reaction 2). A second set of TPD experiments following the initial set from the sputtered surface produced results similar to those found on the fully oxidized surface, suggesting that the sputter-induced damage of this surface is completely healed by annealing and also that the dissociation of acetaldehyde most likely oxidizes the reduced surface. Reaction 3 shows that the bimolecular coupling to produce $C_4H_8$ may also involve the oxidation of $Ti^{3+}$ to $Ti^{4+}$. Desorption of 54 amu indicates further dehydrogenation of $C_4H_8$ and formation of butadiene ($C_4H_6$, $m/e$ = 54) following adsorption of acetaldehyde on the sputter-reduced surface. Similar reductive coupling has also been observed following adsorption of acetaldehyde on the reduced $TiO_2$(001) surface,[8] indicating that reduced Ti cation sites are responsible for the initiation of the coupling reactions.

The proposed reaction mechanism for the formation of symmetric olefin through reductive coupling is not the only one possible. For example, two molecules of acetaldehyde may couple on two oxygen defect sites to give pinacolates ($CH_3$−CHO(a)−(a)OHC−$CH_3$), which would then give the symmetric olefin, such as $C_4H_8$. The $C_2H_4$ may also be produced by dehydration of ethoxides that can be formed by a partial reduction of adsorbed acetaldehyde. Ethoxides, instead of being hydrogenated to give ethanol, may dehydrate to give ethylene.

It is not surprising that aldol condensation was not observed on the reduced $SrTiO_3$ surfaces because aldol condensation takes place through the reduction of an oxidized surface. Previous studies on oxidized and reduced $CeO_2$ surfaces revealed that the reducibility and basicity of the oxidized $CeO_2$ surfaces favor aldolization reactions, whereas the reduced $CeO_2$ is more active for cross-reductive coupling reaction between the adsorbed aldehyde molecules.[34] In our studies there was no evidence that the aldol condensation took place on the fully oxidized $SrTiO_3$-(100) surface, indicating that $Ti^{4+}$ cation sites on the oxidized $SrTiO_3$(100) are not sufficiently activating. The previous studies on the interactions of acetaldehyde with $TiO_2$(001) surfaces, however, indicated that aldol condensation occurs on both {011}- and {114}-faceted $TiO_2$(001) surfaces[6] and that aldol condensation, although a bimolecular reaction, is relatively insensitive to the surface structures based on the comparison of the results obtained from the {011}- and {114}-faceted surfaces. The {011}-faceted surface, in their studies, was thought to be a fully oxidized surface exposing only five-coordinated cations.[6] The STM study,[21] however, showed a certain number of mixed coordination sites on the same surface. Comparing the results obtained in this study with the interpretations of the previous studies, and assuming that the STM results revealed the correct structural information on the {011}-faceted surface, we suggest that the nonuniform cation sites on the fully oxidized surfaces are responsible for the initiation of aldol condensation. The {011}- and {114}-faceted surfaces containing four-, five-, and six-coordinated cations are capable of initiating aldol condensation, whereas the fully oxidized $SrTiO_3$(100) surface lacks unsaturated cation sites and is, therefore, inert to aldol condensation. Thus, the enhanced reactivity of $CH_3CHO$ on the $TiO_2$(100) surfaces can be related to the unique structures of the faceted $TiO_2$(001) surfaces that possess a variety of surface sites, many of which are very active toward the reactions of organic molecules adsorbed on these surfaces.

## 4. Conclusions

Interactions of $CH_3CHO$ with stoichiometric ($TiO_2$-terminated) and reduced $SrTiO_3$(100) surfaces have been studied using temperature-programmed desorption (TPD) and X-ray photoelectron spectroscopy (XPS). $CH_3CHO$ mostly adsorbs molecularly on the stoichiometric surface where no reaction products are observed at temperatures above 400 K. However, decomposition and redox reactions of acetaldehyde occur on

$SrTiO_3$(100) surfaces containing defects created by $Ar^+$ sputtering. Reductive coupling to produce $C_2H_4$ and $C_4H_8$ is the main reaction channel for decomposition of acetaldehyde on the sputter-reduced surfaces of $SrTiO_3$(100). The $Ti^{4+}$ cation sites on $SrTiO_3$(100) surfaces are not capable of initiating surface reactions such as aldol condensation, unlike the $Ti^{4+}$ cations on $TiO_2$(001) surfaces. It was found that the nonuniform $Ti^{4+}$ cation sites are required for aldol condensation. The differences in reactivities between $SrTiO_3$ and $TiO_2$ surfaces presumably originate from the unique geometric and electronic structure of the $SrTiO_3$(100) surfaces.

**Acknowledgment.** This work was supported by the Division of Materials Sciences and the Division of Chemical Sciences, Office of Basic Energy Sciences, U.S. Department of Energy (USDOE). The experiments were performed in the Environmental Molecular Science Laboratories (EMSL), a national scientific user facility located at Pacific Northwest National Laboratory (PNNL) and supported by the U.S. Department of Energy's Office of Biological and Environmental Research. PNNL is a multiprogram national laboratory operated for USDOE by Battelle Memorial Institute under Contract No. DE-AC06-76RLO 1830.

## References and Notes

(1) Sakugawa, H.; Kaplan, I. R. *Atmos. Environ.* **1993**, *27B*, 203.
(2) Roberts, J. M. *Atmos. Enviro.* **1990**, *24A*, 243.
(3) Graedel, T. E.; Mandich, M. L.; Weschler, C. J. *J. Geophys. Res.* **1986**, *91*, 5205.
(4) Altshuller, A. P. *Atmos. Environ.* **1993**, *27A*, 21.
(5) Gopel, W.; Rocker, G.; Freierabend, R. *Phys. Rev. B* **1983**, *28*, 3427.
(6) Idriss, H.; Kim, K. S.; Barteau, M. A. *J. Catal.* **1993**, *139*, 119.
(7) Idriss, H.; Barteau, M. A. *Catal. Lett.* **1992**, *15*, 13.
(8) Idriss, H.; Barteau, M. A. *Catal. Lett.* **1992**, *40*, 147.
(9) Idriss, H.; Pierce, K.; Barteau, M. A. *J. Am. Chem. Soc.* **1991**, *113*, 715.
(10) Wrighton, M. S.; Ellis, A. B.; Wolczanski, P. T.; Morse, D. L.; Abrahamson, H. B.; Ginley, D. S. *J. Am. Chem. Soc.* **1976**, *98*, 2774.
(11) Henderson, M. A. *Surf. Sci.* **1998**, *412/412*, 252.
(12) Yoshimoto, M.; Maeda, T.; Shimozono, K.; Koinuma, H.; Shinohara, M.; Ishiyama, O.; Ohtani, F. *Appl. Phys. Lett.* **1994**, *65*, 3197.
(13) Nishimura, T.; Ikeda, A.; Namba, H.; Morishita, T.; Kida, Y. *Surf. Sci.* **1999**, *421*, 273.
(14) Redhead, P. A. *Vacuum* **1962**, *12*, 203.
(15) Wang, L.-Q.; Azad, S.; Ferris, K. F., to be submitted for publication.
(16) Firment, L. E. *Surf. Sci.* **1982**, *116*, 205.
(17) Chung, Y. W.; Lo, W. J.; Somorjai, G. A. *Surf. Sci.* **1977**, *64*, 588.
(18) Kasowski, R. V.; Tait, R. H. *Phys. Rev. B* **1979**, *20*, 5168.
(19) Tait, R. H.; Kasowski, R. V. *Phys. Rev. B* **1979**, *20*, 5179.
(20) Muscat, J.; Harrison, N. M. *Surf. Sci.* **2000**, *446*, 119.
(21) Poirier, G. E.; Hance, B. K.; White, J. M. *J. Vac. Sci. Technol., B* **1992**, *10* (1), 6.
(22) Tero, R.; Fukui, K.-I.; Iwasawa, Y. *J. Phys. Chem. B* **2003**, *107*, 3207.
(23) Wang, L.-Q.; Ferris, K. F.; Herman, G. S. *J. Vac. Sci. Technol., A* **2002**, *20*, 239.
(24) Rodriguez, J. A.; Azad, S.; Wang, L. Q.; Carcia, J.; Etxeberria, A.; Gonzalez, L. J. *Chem. Phys.* **2003**, *118*, 6562.
(25) Barr, T. L. *J. Vac. Sci. Technol., A* **1991**, *9*, 1793.
(26) Ferris, K. F.; Wang, L.-Q. *J. Vac. Sci. Technol., A* **1998**, *16*, 956.
(27) Wang, L.-Q.; Ferris, K. F.; Herman, G. S.; Engelhard, M. H. *J. Vac. Sci. Technol., A* **2000**, *18*, 1893.
(28) Yamaguchi, Y.; Onishi, H.; Iwasawa, Y. *J. Chem. Soc., Faraday Trans.* **1995**, *91*, 1663.
(29) Idriss, H.; Lusvardi, V. S.; Barteau, M. A. *Surf. Sci.* **1996**, *348*, 39.
(30) Henderson, M. A. *J. Phys. Chem.* **1995**, *99*, 15253.
(31) Wang, L.-Q.; Ferris, K. F.; Shultz, A. N.; Baer, D. R.; Engelhard, M. H. *Surf. Sci.* **1997**, *380*, 352.
(32) (a)Henderson, M. A.; Otero-Tapia, S.; Castro, M. E. *Faraday Discuss.* **1999**, *114*, 313. (b) Henderson, M. A.; Otero-Tapia, S.; Castro, M. E. *Surf. Sci.* **1998**, *412/413*, 252.
(33) Gamble, L.; Jung, L. S.; Campbell, C. T. *Surf. Sci.* **1996**, *348*, 1.
(34) Idriss, H.; Diagne, C.; Hindermann, J. P.; Kiennemann, A.; Barteau, M. A. *J. Catal.* **1995**, *155*, 219.